Proceedings of POWER-2005
2005 ASME Power Conference
Chicago, Illinois, USA, April 5-7, 2005

PWR2005-50070

PROBABILISTIC PERFORMANCE ANALYSIS OF ERODED COMPRESSOR BLADES

A. Kumar*, P. B. Nair, A. J. Keane
Computational Engineering and Design Group
School of Engineering Sciences
University of Southampton
Southampton, SO171BJ, UK

S. Shahpar
Aerothermal Methods
Rolls-Royce plc
PO Box 31
Derby, DE248BJ, UK.

ABSTRACT

This paper presents a probabilistic analysis of the effect of erosion on the performance of compressor fan blades. A realistic parametric CAD model is developed to represent eroded blades. Design of Experiments (DOE) techniques are employed to generate a set of candidate points, which are combined with a parametric geometry modeling and grid generation routine to produce a hybrid mesh. A multigrid Reynolds-Averaged Navier Stokes (RANS) solver HYDRA with Spalart Allmaras turbulence model is used for Computational Fluid Dynamics (CFD) simulations. The data generated is used to create a surrogate model for efficient uncertainty propagation. This method is applied to a typical Rolls Royce compressor fan blade section. Monte Carlo Simulation, using the surrogate model, is executed for the probabilistic analysis of the compressor fan blade. Results show upto 5 % increase in pressure loss for the eroded compressor fan blades.

INTRODUCTION

The behaviour of compressor fan blades is central to the performance of modern gas turbine engines. Such fan blades have subtle aerodynamic shapes designed after decades of research and insight. However, airfoils inevitably exhibit deviation from their intended shape and size. Geometric uncertainty may be introduced for instance, by manufacturing errors, icing or operational wear and damage.

The geometry variations in airfoils due to erosion, manufacturing errors and icing are distinct and require different modeling tools. Manufacturing errors introduce subtle and smooth shape changes to the desired airfoil shape and can cause an increase or decrease in the airfoil profile. Icing is deposition of ice on the airfoil surface and always causes protrusion. Erosion on the other hand leads to blade surface deterioration and causes loss of material in the original airfoil. Hence for modeling eroded geometries, a tool that can model local dents in the original airfoil shape is required.

The effect of geometric variability, primarily caused by manufacturing errors, on the performance of axial compressors has been studied by Garzon et al in [1]. The probabilistic model used by them was based on Principal-Component Analysis [2] of the blade surface measurements. They employ a full scale Monte Carlo Simulation to understand the effects of manufacturing uncertainties on the aerodynamic and aerothermal properties of high-pressure axial compression systems. Their study suggests that the overall compressor efficiency could deteriorate by approximately 1% due to blade passage effects arising from representative manufacturing variability.

Bragg et al [3,4] have studied the aerodynamic performance of airfoils with added ice shapes. They have conducted numerical studies to investigate the effect of leading-edge ice shapes and simulated ridge ice shapes on the aerodynamic behaviour of airfoils and wings, over a range of Reynolds numbers and Mach numbers. The effect of ice shape size and location has been studied on the stall condition, lift and drag values by Pan et al [5]. They have validated their RANS based studies with experimental data and suggested use of higher fidelity methods, such as Large

*ak3@soton.ac.uk

Copyright © 2005 by ASME

Eddy Simulations or Detached Eddy Simulations, for post-stall analysis where the flow tends to be unsteady and separated.

During operation, compressor fan blades are exposed to a number of erosion processes [6]. This can lead to reduction of the blade chord, alteration in the shape and increase in the surface roughness [7, 8]. In their study Tabakoff et al use a semi-empirical erosion model, derived from erosion tests of material samples at different particulate flow conditions, to predict the blade erosion patterns and locations. Roberts [9] has shown that geometric variability in the form of leading edge erosion in compressor airfoils may account for an increase of 3 % or more on the thrust specific fuel consumption.

In this work a novel parametric CAD representation of eroded compressor blade sections is developed using Hicks-Henne bump functions [10]. Since running a full scale Monte Carlo Simulation [11] would be computationally very expensive, DOE techniques [12] are used for the probabilistic analysis. LP_τ sampling [13] is used to create the DOE candidate points. This is combined with PADRAM [14] (Parametric Design and Rapid Meshing) to generate a hybrid C-O-H mesh. The multigrid solver HYDRA with four multigrid levels is used to carry out CFD simulations at the DOE candidate points. The Spalart Allmaras model is used for modeling turbulence.

The present study uses a Gaussian stochastic process model as a surrogate to the computationally expensive CFD simulations for probabilistic analysis. Jones and Ong et al [15, 16] have discussed the use of surrogate models for optimization involving computationally expensive problems. A Bayesian surrogate modeling technique [17] is used here to construct an interpolant with the data generated from the DOE runs. It creates a hypersurface which approximates the pressure loss as a function of the geometric variables. This is further used to understand the effect of each geometric parameter on the performance of the airfoil. Finally, Monte Carlo Simulation (MCS) with 10,000 samples is executed to perform a probabilistic analysis of the effect of erosion on the pressure loss of compressor fan blades.

The remainder of the paper is organized as follows. In the next section, we discuss how the eroded compressor blade geometry is parametrized and flow analysis is conducted. This is followed by the theoretical and computational aspects of surrogate modeling approach. The last two sections present the numerical studies and conclusions.

MODELING AND PARAMETRIZATION

We consider a typical Rolls-Royce compressor fan blade geometry section for our CFD analysis. The Rolls-Royce propriety code PADRAM, a parametric design and meshing routine is employed for creating the geometry and grid generation. PADRAM makes use of both transfinite interpolation and elliptic grid generation to generate hybrid C-O-H meshes. An orthogonal body fitted O mesh is used to capture the viscous region of the airfoil whilst an H mesh is used near the boundary where stretched cells are required, for example in the wake region. After Grid refinement studies we select a mesh of the order of 28,000 cells. Figure 1 shows a typical compressor fan blade section geometry with the CFD mesh.

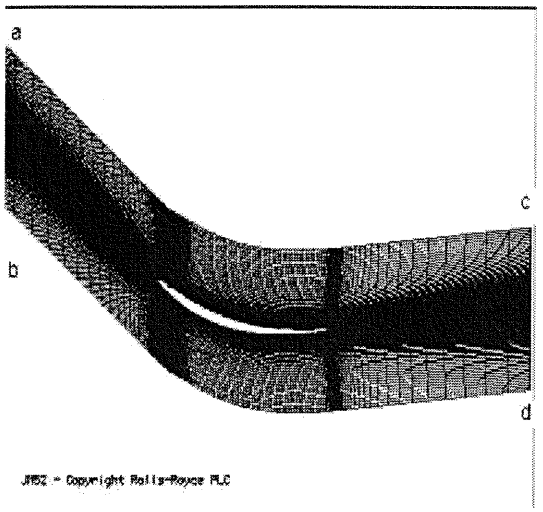

Figure 1. A typical C-O-H mesh used for CFD analysis

In Figure 1 *abdc* is the CFD domain where boundary *ab* is the inlet and boundary *cd* is the exit. A non-linear, unstructured viscous flow solver HYDRA [18] is used for the CFD simulation. It solves the steady Navier-Stokes equations with the Spalart-Allmaras turbulence model. To accelerate the convergence to steady-state it uses preconditioning and multigrids [19]. A four level multigrid is used for the present simulations. The inlet boundary conditions for the CFD analysis are Total temperature = 290 Kelvin, Total Pressure = 63400 Pascal, Whirl Angle = -37.28 Degrees and the outlet boundary condition is Static Pressure = 52000 Pascal. An initial uniform flow condition with Density = 0.7675 kg/m^3, Velocity = 0 and Pressure = 66932 Pascal is considered. The converged CFD solution is used to calculate the pressure loss at the nominal geometry. The equation for the pressure loss is:

$$Loss = \frac{P_{inlet} - P_{exit}}{P_{inlet}} \times 100. \quad (1)$$

where P_{inlet} is the total pressure at the inlet and P_{exit} is the total pressure at the exit.

The next step is to develop a parametric model of the eroded compressor blade section. Erosion leads to blade surface deterioration and causes a depression in the original airfoil. Hence for

Copyright © 2005 by ASME

modeling eroded geometries, a tool that can model local dents in the original airfoil shape is required. Hicks Henne functions provide a flexible tool to model local variation in the form of bumps. Erosion patterns observed in compressor fan blades can be very complex. A combination of piece-wise cubic polynomial and Hicks-Henne function is used here to create a simple but realistic model of the erosion patterns. The eroded compressor fan blade section is parametrized in terms of the location, height and the width of the eroded section. The Hicks-Henne functions can be expressed as:

$$b(x) = A\left[sin\left(\pi x^{\frac{log5}{log t_1}}\right)\right]^{t_2}, 0 \leq x \leq 1. \qquad (2)$$

Here, A is the maximum bump magnitude, t_1 locates the maximum of the bump at $x = t_1$, and t_2 controls the width of the bump. This model is combined with the parametric model present in PADRAM. Clustering functions and continuity checks are employed to prevent negative volumes and high skewness during grid generation. The aim is to construct a robust automated geometry modeler and grid generator which can be combined with the CFD simulation code HYDRA for the probabilistic analysis of the performance of the eroded compressor fan blade geometries. A zoomed in view of a typical eroded geometry, with erosion in the leading edge, with the CFD mesh, is shown in figure 2.

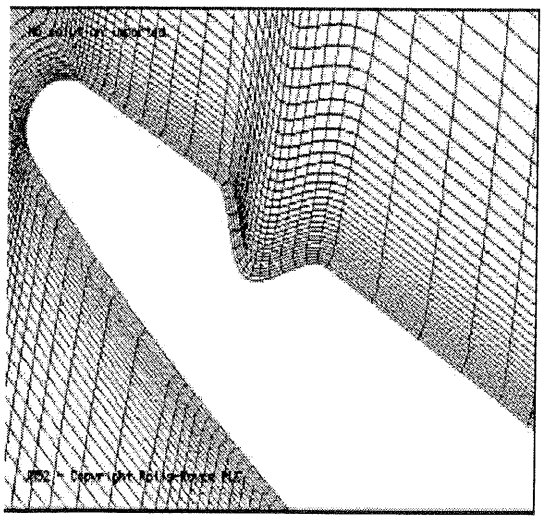

Figure 2. A typical PADRAM C-O-H mesh used for CFD analysis

SURROGATE MODELING

In probabilistic analysis the computational cost involved in solving high-fidelity simulation models many times over is very high. Surrogate modeling uses the basic idea of analyzing an initial set of design points to generate data which can be used to construct approximations of the original high fidelity model. The high-fidelity model CFD simulation in this study can be represented by a functional relationship $y = f(\mathbf{x})$, where $\mathbf{x}$ is the vector of inputs to the simulation code and y is the output. The objective is to construct an approximate model $\hat{y} = \hat{f}(\mathbf{x}, \alpha) \approx f(\mathbf{x})$, that is computationally cheaper to evaluate. α is a vector of undetermined hyperparameters which is estimated by employing a black-box approach [15] to the input-output data. In general, black-box surrogate modeling involves the following steps: (1) data generation, (2) model structure selection, (3) parameter estimation and (4) model validation.

Data Generation

A surrogate modeling approach needs a set of training data and the quality of the approximate model crucially depends on the location of these training points. Design of experiments (DOE) techniques offer a way to choose the training points so that the maximum quantity of information can be extracted about the underlying input-output relationship. As computer experiments are deterministic, it is important to choose the training points which fill the design space in an optimal sense [20]. The Monte Carlo Simulation (MCS) technique is among the most robust and simple techniques, wherein the basic idea is to employ a random number generator to sample the design space. However MCS is used as the method of last resort as the points are not essentially space filling and the computational cost involved with high fidelity models can be prohibitively high. Mckay et al [21] proposed the Latin hypercube sampling (LHS) technique, which is a computationally cheaper alternative to MCS for designing computer experiments. The underlying idea is to divide the design space into regions of equal probability and generate pseudo random points, such that no two points lie in the same bin. Other commonly used methods are stratified MCS, Orthogonal arrays and minimum discrepancy sequences. We use one of the minimum discrepancy methods based on Sobol sequences [22] also known as the LP_τ method. LP_τ sampling [13] is based on uniformly distributed sequences in space and gives a mechanism for generating points in n-dimensional space which are uniformly distributed.

Model Structure Selection

The next step in the surrogate modeling process is to select the model structure. In practice one can use a parametric or non-parametric model. In a parametric model once the model parameters are estimated using the training dataset, the dataset is no longer needed for predicting the output at a new point. Typ-

Copyright © 2005 by ASME

ical example of parametric models are polynomial models [23]. A non-parametric model requires the training dataset even after the undetermined parameters have been evaluated. Kernel methods [24] such as radial basis functions (RBF), support vector machines and Gaussian process models are examples of such models. Parametric models are easier to implement and facilitate the interpretation of the relationship between input-output data, but they do not perform very well when the underlying relationship is complex. The next decision of using a regression or an interpolation model depends on the nature of the dataset. Physical experiments usually contain some random noise in their datasets and hence regression techniques are widely used there. Unlike physical experiments, computer experiments are deterministic with no random noise and theoretically the interpolation models seem more appropriate.

In our study we use a Gaussian stochastic process model to build the surrogate model. The foundations of this method were developed in the field of geostatistics, where this model is referred to as Kriging and has been in use since the early 1960's [25]. It is also widely used in the neural network community where it is referred to as Gaussian process regression [26, 27]. The model structure typically used in stochastic process approximation of the relationship $y = f(\mathbf{x})$ can be compactly written as

$$Y(\mathbf{x}) = \beta + Z(\mathbf{x}), \tag{3}$$

where β is an unknown hyperparameter to be estimated from the data and $Z(\mathbf{x})$ is a Gaussian stochastic process with zero mean and covariance

$$\mathrm{Cov}(Z(\mathbf{x},\mathbf{x}')) = \Gamma(\mathbf{x},\mathbf{x}') = \sigma^2{}_z R(\mathbf{x},\mathbf{x}'). \tag{4}$$

In other words, the observed outputs of the simulation code $\mathbf{y} = \{y^1, y^2, ..., y^l\}$ are assumed to be realizations of a Gaussian random field with mean β and covariance Γ. Here $R(.,.)$ is a parametrized correlation function that can be tuned to the training dataset and $\sigma^2{}_z$ is the so called process variance.

A commonly used choice of covariance function is the stationary family which obeys the product correlation rule [20].

$$R(\mathbf{x}^1,\mathbf{x}^2) = \prod_{j=1}^{p} exp(-\theta_j |\mathbf{x}_j^1 - \mathbf{x}_j^2|^{p_j}), \tag{5}$$

where $\theta_j \geq 0$ and $1 < p_j \leq 2$ are the hyperparameters. In the present study we have chosen $p_j = 2$ assuming that the underlying function being modeled is infinitely differentiable and smooth. The values of the hyperparameter θ can be used to understand the relative importance of each parameter on the performance of the airfoil. Hence θ_j, which is the value corresponding to the jth parameter, is an indicator of the its influence on the airfoil performance. It is possible to tune the parameters p_j to the data which allows for the possibility of modeling functions which are discontinuous. In theory, the choice of an optimal covariance function is dependent on the data. However, in practice it has been found that the parametrized covariance function in equation (3) offers sufficient flexibility for modeling smooth as well as nonlinear functions [17]. If a Gaussian process prior over functions is used, the posterior process is also Gaussian. Hence using standard statistical results from Bayesian inferencing, the posterior mean and covariance can be stated as

$$\hat{y}(\mathbf{x}) = \beta + \tau(\mathbf{x})^T \mathbf{R}^{-1}(\mathbf{y} - \mathbf{1}\beta), \tag{6}$$

and

$$C(\mathbf{x},\mathbf{x}') = \sigma_z{}^2 \left(R(\mathbf{x},\mathbf{x}') - \tau(\mathbf{x})^T \mathbf{R}^{-1} \tau(\mathbf{x}') \right). \tag{7}$$

Here $\mathbf{R}$ is the correlation matrix whose ijth element is calculated as $R(\mathbf{x}^{(i)},\mathbf{x}^{(j)})$ and $\tau = \{R(\mathbf{x},\mathbf{x}^{(1)}), R(\mathbf{x},\mathbf{x}^{(1)}), ..., R(\mathbf{x},\mathbf{x}^{(1)})\}^T \in \mathbb{R}^n$ and $\mathbf{1} = \{1, 1, ..., 1\} \in \mathbb{R}^n$. This approach finally leads to an approximation of the computational model as a multidimensional Gaussian random field. The randomness in equation (7), given by posterior variance $\sigma^2(\mathbf{x}) = C(\mathbf{x},\mathbf{x}')$, can be interpreted as an estimate of the uncertainty involved in predicting the output at any new points using the given finite dataset.

Parameter Estimation

After choosing an appropriate covariance function for the surrogate model the next task at hand is to estimate the set of unknown model parameters. The covariance function Γ can be parametrized in the term of vectors $\theta = \{\theta_1, \theta_2, ..., \theta_p\}$. Given the training dataset, we need to estimate θ and the other hyperparameters β and $\sigma_z{}^2$. Martin et al [28] have compared Maximum Likelihood Estimation (MLE) and Cross-Validation (CV) technique for estimating the parameters. Here we use the MLE technique as proposed in the Design and Analysis of Computer Experiments (DACE) [20]. The MLE approach leads to those values of the undetermined parameters that are most likely to have generated the training dataset. For the Gaussian process interpolation, since we assume that the observed outputs have a Gaussian distribution, the likelihood function can be written as

$$(2\pi)^{-n/2} \sigma_z{}^{-n} |\mathbf{R}|^{-1/2} exp\left(-\frac{1}{2\sigma_z{}^2} (\mathbf{y} - \mathbf{1}\beta)^T \mathbf{R}^{-1} (\mathbf{y} - \mathbf{1}\beta) \right). \tag{8}$$

Copyright © 2005 by ASME

Hence, the negative log-likelihood function to be minimized becomes

$$L(\theta,\beta,\sigma_z^2) = -\frac{1}{2}\left[nln\sigma_z^2 + ln|\mathbf{R}| + \frac{1}{2\sigma_z^2}(\mathbf{y}-\mathbf{1}\beta)^T\mathbf{R}^{-1}(\mathbf{y}-\mathbf{1}\beta)\right]. \tag{9}$$

By taking the derivative of the log-likelihood function with respect to β and σ_z^2 and equating them to zero, we get a closed form solution for the optimal values of β and σ_z^2 as

$$\hat{\beta} = (\mathbf{1}^T\mathbf{R}^{-1}\mathbf{1})^{-1}\mathbf{1}^T\mathbf{R}^{-1}\mathbf{y}, \tag{10}$$

and

$$\hat{\sigma_z^2} = \frac{1}{n}(\mathbf{y}-\mathbf{1}\beta)^T\mathbf{R}^{-1}(\mathbf{y}-\mathbf{1}\beta). \tag{11}$$

A closed-form solution does not exist for θ, requiring an iterative optimization procedure to minimize L as a function of θ. For a given value of θ, estimates of β and σ_z^2 can obtained using equation (10) and (11), respectively. These computed values of β and σ_z^2 can be substituted into equation (9) to calculate the log-likelihood function. In principle, any standard optimization routine can be employed to compute the maximum likelihood estimate of θ.

Model Validation

To assess the quality of our surrogate model we need to perform validation studies. This assessment study can be performed in a number of ways, two common methods are : (1) the accuracy of predicting the output at a number of additional points and (2) a leave-one-out type cross-validation procedure. The first method can become computationally prohibitive for high-fidelity models such as CFD simulation of a geometry with high mesh size. A cross-validation procedure which does not need additional observation data can be a computationally cheap alternative. This method involves leaving the ith training point out and computing the posterior mean at the point $\hat{y}_{-i}(\mathbf{x})$. By plotting the computed values against the original values from the training dataset, the quality of the surrogate model can be assessed. In a recent study, Meckesheimer et al [29] noted that the leave-one-out procedure may significantly underestimate the actual prediction error and suggested that a k-fold cross-validation scheme (with $k = 0.1n$ or $\sqrt{n}$) may be better a indicator of the model quality.

Another measure of the quality of the Gaussian stochastic surrogate model would be to validate our basic assumption, that a Gaussian process prior is appropriate for the CFD simulation code used as a black box here. Jones et al [15] have discussed the use of Standardized Cross-Validated Residual (SCVR) which is defined as

$$SCVR_i = \frac{y^{(i)} - \hat{y}_{-i}(\mathbf{x}^{(i)})}{\sigma_{-i}^2(\mathbf{x}^{(i)})}, i = 1,2,...,n, \tag{12}$$

where $\hat{y}^{(i)}(\mathbf{x})$ and $\sigma_{-i}^2(\mathbf{x})$ denote the mean and variance of the metamodel prediction at a point $\mathbf{x}$ without using the ith training point. $SCVR_i$ can be computed for all the training points by removing the contribution of the corresponding points from the correlation matrix $\mathbf{R}$. Here we can also use an additional validation dataset and calculate the $SCVR_i$ values.

NUMERICAL STUDIES

To estimate the parameters of the surrogate model, we carry out a 50 point LP_τ DOE survey over the values of the erosion parameters $[location, width, height]$. The parameters of the eroded geometry are specified by upper and lower bounds. Figure 3 shows a few erosion patterns constructed by the parametric model.

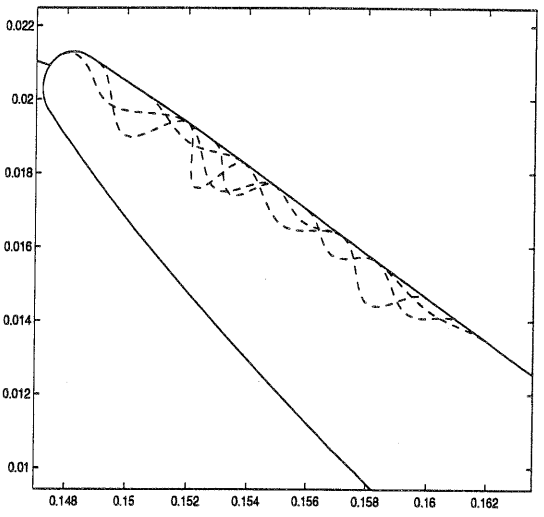

Figure 3. Example of Erosion patterns Constructed by the Parametrized Model

The automated grid generator and CFD simulator are run to evaluate the pressure loss at each design point. The hyperparameters $\theta, \beta, \sigma_z^2$ are evaluated using a hybrid Genetic Algorithm (GA) and Dynamic Hill Climbing (DHC) search method. The scatter plot of the normalized values of pressure loss are shown in figure 4. It can be observed that the pressure loss for most of the eroded geometries have deteriorated. A few geometries with

Copyright © 2005 by ASME

subtle shape changes had an improved performance as compared to the nominal geometry.

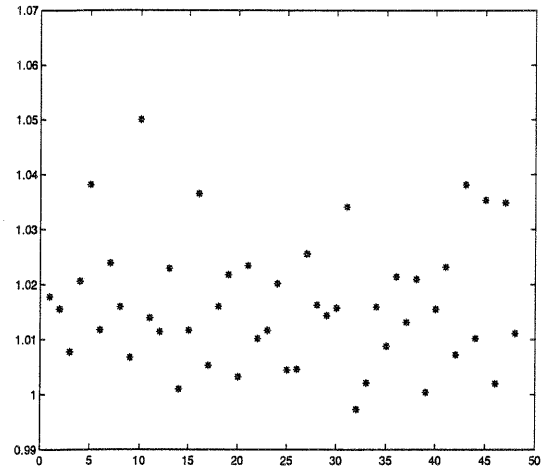

Figure 4. The Scatter Plot of Normalized Pressure Loss

The quality of the surrogate model is illustrated in figures 5 and 6. Figure 5 is a plot of the posterior mean value predicted using leave-one-out validation test versus the observed values. The regression coefficient for this test was $R^2 = 0.9023$. In figure 6 we observe that some of the $SCVR_i$ values do not lie within $[-3\sigma, +3\sigma]$. A simple way to improve the surrogate model is to add more points to the DOE dataset. A better method for improving the performance of the surrogate model would be to add points where the observed $SCVR_i$ values are high.

Here we increase the observed dataset by adding design points created using a LHS technique. Figures 7, 8 show the plot of posterior mean and $SCVR_i$ values predicted by the leave-one-out method used on the new training dataset. The plot of the posterior mean value predicted using leave-one-out validation method vs the observed values using the surrogate model built using the new dataset indicates a better model. The regression coefficient for the new prediction is $R^2 = 0.9395$. It can also be observed that most of the $SCVR_i$ in figure 8 lie within the $[-3\sigma, +3\sigma]$ bracket.

Having established the quality of the surrogate model we use it to study the underlying behaviour of erosion parameters on the blade at modest cost. A 10,000 point Monte Carlo simulation is run on the surrogate model to generate the probability distribution of the pressure loss. The values of the parameters $[location, width, height]$ are defined to lie within a prescribed lower and upper bound. A uniform distribution of the erosion parameters $[location, width, height]$ is assumed for the probabilistic analysis. The histogram for the pressure loss evaluated using MCS is shown in figure 9. The MCS using the surrogate model takes a few minutes for carrying out 10,000 evaluations on Intel(R) Xeon(TM) CPU 3.06GHz dual processor machine.

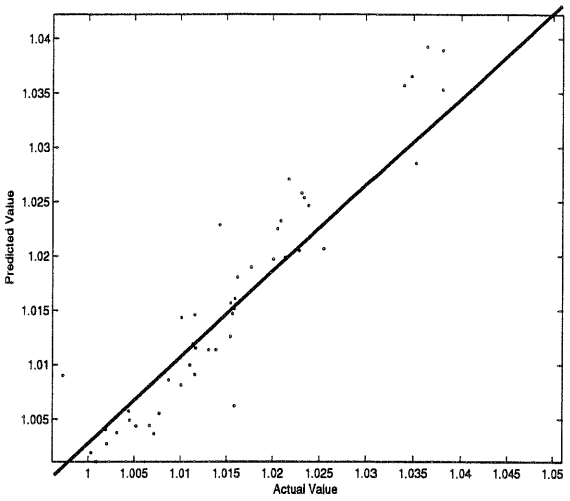

Figure 5. Predicted Posterior Mean Values Versus Observed Values with $R^2 = 0.9023$

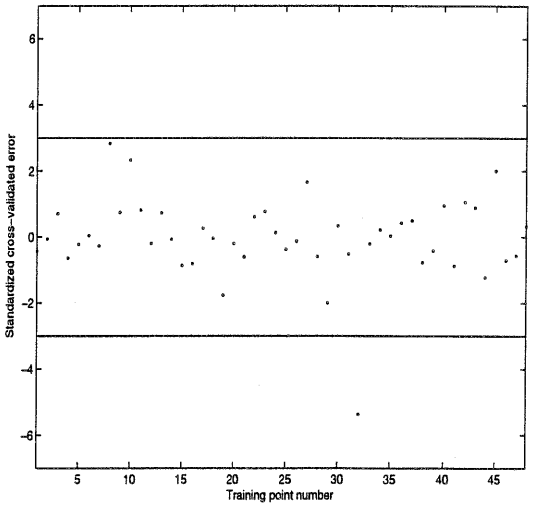

Figure 6. $SCVR_i$ Values Predicted with Leave-One-Out Validation

The values of the hyperparameter $\theta = [\theta_{location}, \theta_{width}, \theta_{height}]$ can be used to understand the relative importance of the erosion parameters on the pressure loss. We found the importance factors corresponding to $[location, width, height]$ to be $[0.6581, 0.2300, 0.1119]$ respec-

Copyright © 2005 by ASME

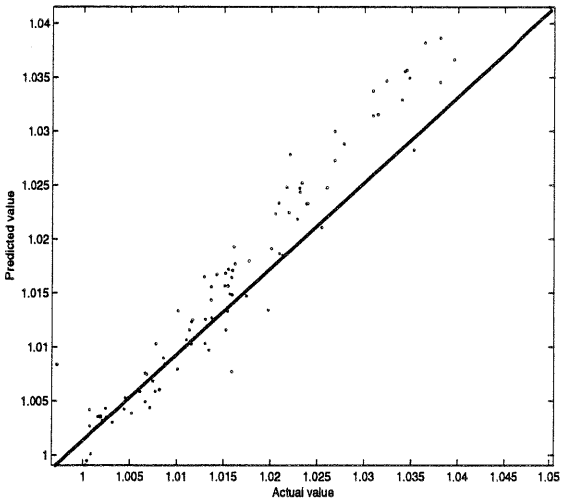

Figure 7. Predicted Posterior Mean Values Versus Observed Values with New Dataset and $R^2 = 0.9395$

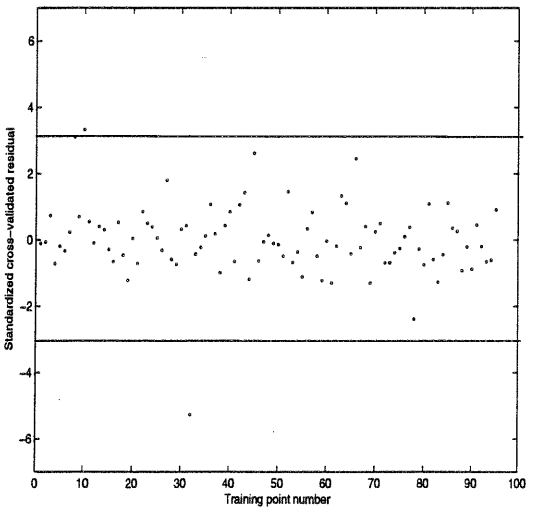

Figure 8. $SCVR_i$ Values Predicted with Leave-One-Out Validation with Larger Dataset

tively, indicating that the *location* and *width* have more influence on the pressure loss. Figure 10 shows the contours of pressure loss for variations of location and width. The values of location and width have been normalized, so that a value of location close to zero indicates proximity to the leading edge and a value close to unity indicates that the erosion is located further toward the trailing edge. The contour plot suggests that the performance of a compressor fan blade deteriorates as the erosion is located

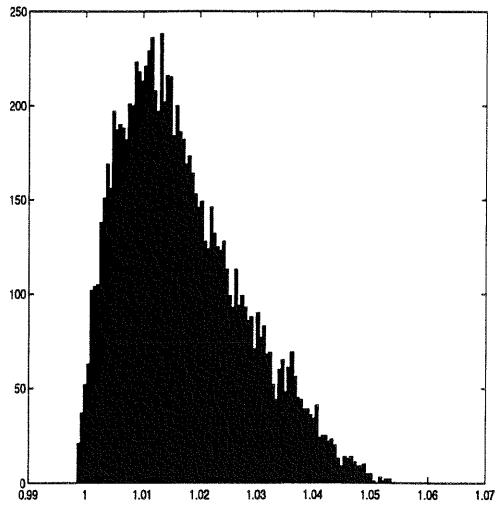

Figure 9. Probability Distribution of the Pressure Loss using MCS

nearer to the leading edge as might be expected. Similarly, for wider erosion patterns the pressure loss is higher. It is interesting that erosion depth appears least significant.

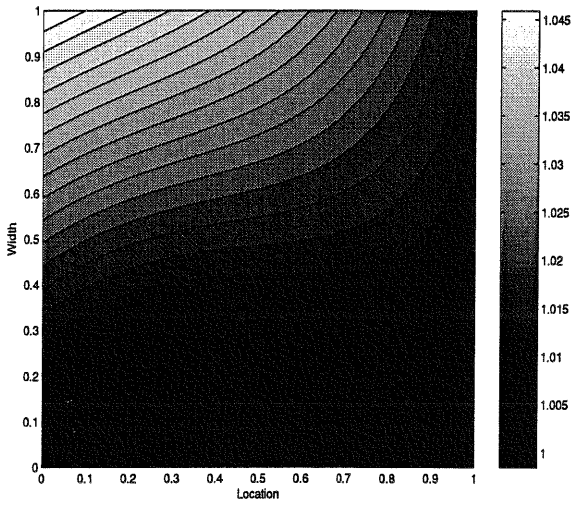

Figure 10. Contour Plot of Pressure Loss against Location and Width

CONCLUSIONS

In this study we have presented a new way to model and parametrize an eroded blade geometry. This model has been

Copyright © 2005 by ASME

used for a probabilistic analysis of the effect of erosion parameters on the pressure loss of a typical high-pressure Rolls-Royce compressor fan blade geometry. A robust automatic geometric modeler and grid generator has been employed to create the geometry and high quality CFD mesh. To reduce the computational costs associated with the probabilistic analysis of high-fidelity simulation systems, we replaced the CFD simulation code by a black-box based surrogate model. A Gaussian stochastic process model (Krig) was developed using a training dataset created by a combination of LHS and LP_τ based DOE techniques. The model was assessed using leave-one-out methods, and consequently improved by using additional dataset points. Finally a Monte Carlo Simulation was executed to understand the effect of each parameter $[location, height, width]$ on the pressure loss of the compressor fan blade section.

The analysis shows upto 5% increase in pressure loss for the eroded geometry types. It was also observed that some eroded geometries performed better. The analysis suggests that the location and width of the erosion pattern have more influence on the performance of the airfoil compared to depth. This analysis could also be used to understand the critical locations, width and heights of the erosion patterns.

The parametric model used here could also be extended to model manufacturing errors using combinations of Hicks-henne functions. The work could be further extended to study the effect of erosion on a cascade of compressor fan blades and multistage systems. In future work we propose to use the approach set out here, to allow the impact of erosion/damage to be included alongside nominal performance, during shape optimization in a multi-objective setting. This work will be further extended for robust design against erosion/damage of the compressor fan blade.

ACKNOWLEDGMENT

This work was supported by the University Technology Partnership for Design, a collaboration between Rolls-Royce Plc., BAE Systems and the Universities of Sheffield, Cambridge and Southampton.

REFERENCES

[1] Garzon, V. E., 2003. *Probabilistic Aerothermal Design of Compressor Airfoils.* PhD Thesis, Massachusetts Institute of Technology.

[2] Garzon, V. E., and Darmofal, D. L., 2003. "Impact of geometric variability on axial compressor performance". *ASME Turbo Expo GT2003-38130*.

[3] Bragg, M. B., 1986. "An experimental study of the aerodynamics of a naca0012 airfoil with simulated glaze ice". *AIAA-85-0484*.

[4] Bragg, M. B., and Khodadoust, A., 1989. "Effect of simulated glaze ice on a rectangular wing". *AIAA-89-0750*.

[5] Pan, J., Loth, E., and Bragg, M. B., 2003. "RANS simulation of airfoils with ice shapes". *AIAA 2003-0729*.

[6] Metwally, M., Tabakoff, W., and Hamed, A., 1995. "Blade erosion in automotive gas turbine engine". *Journal of Engineering for Gas Turbine and Power,* **117** , pp. 213–219.

[7] Balan, C., and Tabakoff, W., 1984. "Axial flow compressor performance deterioration". *AIAA 84-2108*.

[8] Hamed, A., Tabakoff, W., and Singh, D., 1998. "Modeling of compressor performance deterioration due to erosion". *International Journal of Rotating Machinery,* **4** , pp. 243–248.

[9] Roberts, W. B., 1984. "Axial compressor performance restoration by blade profile control". *AIAA-84-GT-232, ASME*.

[10] Hicks, R. M., and Henne, P., 1978. "Wing design by numerical optimisation". Journal of Aircraft, **15** (7) , pp. 407–412.

[11] Hurtado, J. E., and Barbat, A. H., 1998. "Monte carlo techniques in computational stochastic mechanics". Arch. Comput. Meth. Engrg, **5** (1) , pp. 3–30.

[12] Gentle, J. E., 1998. *Random Number Generator and Monte Carlo Methods.* Springer, Berlin.

[13] Statnikov, R. B., and Matusov, J. B., 2002. *Multicriteria Analysis in Engineering.* Kluwer Academic Publishers.

[14] Shahpar, S., and Lapworth, L., 2003. "Parametric design and rapid meshing systems for turbomachinery optimisation". *ASME-GT2003-38698*.

[15] Jones, D. R., Schonlau, M., and Welch, W. J., 1998. "Efficient —global optimization of expensive black-box functions". Journal of Global Optimization, **13** (4) , pp. 455–492.

[16] Ong, Y. S., Nair, P. B., and Keane, A. J., 2003. "Evolutionary optimisation of computationally expensive problems via surrogate modeling". AIAA Journal, **40** (4) , pp. 687–696.

[17] Nair, P. B., Choudhary, A., and Keane, A. J., 2001. "A bayesian framework for uncertainty analysis using deterministic black-box simulation code". *AIAA-2001-1676*.

[18] Moinier, P., 1999. *Algorithm developments for an Unstructured Viscous Flow Solver.* PhD Thesis, Oxford University, Oxford.

[19] Moinier, P., Muller, J. D., and Giles, M. B., 1999. "Edge-based multigrid and preconditioning for hybrid grids". *AIAA-99-3339*.

[20] Sacks, J., Welch, W. J., Mitchell, T. J., and Wynn, H. P., 1989. "Design and analysis of computer experiments". Statistical Sciences, **4** (4) , pp. 409–435.

[21] Mckay, M. D., Conover, W. J., and Beckman, R. J., 1979. "A comparison of three methods for selecting values of input variables in the analysis of output from a computer code". *Technometrics,* **21** , pp. 239–245.

[22] Sobol, I. M., 1994. *A Primer for the Monte Carlo Method.* CRC Press, Boca Raton.

Copyright © 2005 by ASME

[23] Myers, R. H., and Montgomery, D. C., 2002. *Response Surface Methodology: Process and Product Optimization Using Designed Experiments*. Wiley Series in Probability and Statistics, John Wiley Sons, New York.

[24] Vapnik, V., 1998. *Statistical Learning Theory*. Wiley, New York.

[25] Matheron, G., 1963. "Principles of geostatistics". *Economic Geology*, **58** , pp. 1246–1266.

[26] Neal, R. M., 1996. *Bayesian Learning for Neural Networks*. Springer.

[27] MacKay, D. J. C., 1997. Guassian processes - a replacement for supervised neural networks. Tutorial lecture Notes for NIPS, at `http://www.inference.phy.cam.ac.uk/mackay/abstracts/gp.html`.

[28] Martin, J. D., and Simpson, T. W., 2004. "On the use of kriging models to approximate deterministic computer models". ASME International Design Engineering Technical Conference and Computer and Information in Engineering Conference. DETC2004/DAC-57300.

[29] Meckesheimer, M., Booker, A. J., Barton, R. R., and Simpson, T., 2002. "Computationally inexpensive metamodel assessment strategies". AIAA Journal, **40** (10) , pp. 2053–2060.

Copyright © 2005 by ASME